CrystEngComm

PAPER

View Article Online
View Journal

Cite this: DOI: 10.1039/c5ce00731c

Structure analysis of a BEC-type germanosilicate zeolite including the location of the flexible organic cations in the channels†

S. Smeets,[a] L. Koch,[a] N. Mascello,[a] J. Sesseg,[a] L. B. McCusker,*[a] M. Hernández-Rodríguez,[b] S. Mitchell[b] and J. Pérez-Ramírez[b]

Received 15th April 2015,
Accepted 2nd June 2015

DOI: 10.1039/c5ce00731c

www.rsc.org/crystengcomm

A **BEC**-type zeolite (polymorph C of zeolite beta) with low germanium content (Si : Ge = 5.1) has been synthesised using the flexible linear diquaternary cationic form of pentamethyldiethylenetriamine (2,2′-(methylazanediyl)bis(*N*,*N*,*N*-trimethylethanammonium) as the organic structure-directing agent (SDA). The distribution of germanium within the framework and the location of the SDA within the pores have been determined by analysing synchrotron X-ray powder diffraction data collected on the as-synthesised form. The findings, which are corroborated by ^{13}C and ^{19}F NMR data, indicate that the structure of the SDA is retained during the synthesis and that the Ge atoms occupy only sites in the double 4-ring. Although the **BEC** framework structure has a three-dimensional 12-ring channel system, the SDA molecules are found to orient themselves in two dimensions along the channels running parallel to the *a* and *b* axes.

Introduction

There is a continued strong interest in understanding the synthesis of zeolites, in particular the conditions that deliver a particular framework type, polymorph, composition, nanostructure, *etc.* Because of the high complexity of the self-assembly processes involved, this type of information is typically gathered through structured screening programs. As part of such a study, we isolated a germanosilicate with the **BEC**-type framework structure.

Polymorph C of zeolite beta (framework type **BEC**)[1] has an interesting history. The existence of this polymorph was first hypothesised in 1988. It was expected to offer good mass-transfer properties because of its 3-dimensional network of linear 12-ring channels,[2] but it took 12 years before the first report of its structure appeared. That material, FOS-5, was synthesised in the form of a pure germanate.[3] It was later attained as a germanosilicate (ITQ-17)[4] with Si : Ge ratios of up to 30, and then as a pure silicate, initially as an overgrowth on zeolite beta,[5] and subsequently as a single-phase material, by including K^+ ions in the reaction mixture.[6] More recently, a titanium silicate version was also reported.[7] A series of organic structure-directing agents (SDAs) can be used to produce the pure polymorph,[8] and these, with the exception of tetraethylammonium, all contain fairly large ($C_{11}+$) and rigid cyclic and polycyclic N-heterocycles.

Germanium is known to play a stabilising role in the formation of double 4-rings (*d4r*) in germanosilicates,[9–11] enabling the formation of polymorph C, which contains a plethora of *d4r* units, even in the absence of fluoride media. However, the incorporation of Ge into a zeolite framework typically leads to a reduction in thermal and hydrothermal stability, and therefore it is desirable to minimise its content. Some researchers have developed experimental methods to overcome this structural weakness, by replacing Ge with Al,[12] Si,[13] or Ti[14] in a post-synthesis treatment. Others turn it to advantage, by exploiting the preferential occupation of Ge in the *d4r* units to invoke an inverse sigma transformation to create high-silica zeolites with new frameworks.[15–17]

The **BEC**-type germanosilicate obtained in this study (hereafter referred to as Ge-BEC) has a low Ge content (Si : Ge = 5.1) and was synthesised using the diquaternary cation (2,2′-(methylazanediyl)bis(*N*,*N*,*N*-trimethylethanammonium, denoted as HM-dq) as the SDA (Fig. 1a). Early research demonstrated that this flexible linear molecule could promote the formation of a number of different zeolites, including ZSM-5, mordenite, ZSM-39, ZSM-48, ZSM-51 and gismondine.[18,19] As this represents a new approach to the synthesis of zeolite beta polymorph C, it was of interest to investigate how the different synthesis conditions and lower Ge content affected the Ge distribution in the framework, and to determine where

[a] *Laboratory of Crystallography, D-MATL, ETH Zurich, CH-8093 Zurich, Switzerland. E-mail: mccusker@mat.ethz.ch*
[b] *Institute for Chemical and Bioengineering, D-CHAB, ETH Zurich, CH-8093 Zurich, Switzerland*

† Electronic supplementary information (ESI) available: Results of the TGA and ^{19}F NMR, and crystallographic information file (cif) of the refined structure of Ge-BEC. See DOI: 10.1039/c5ce00731c

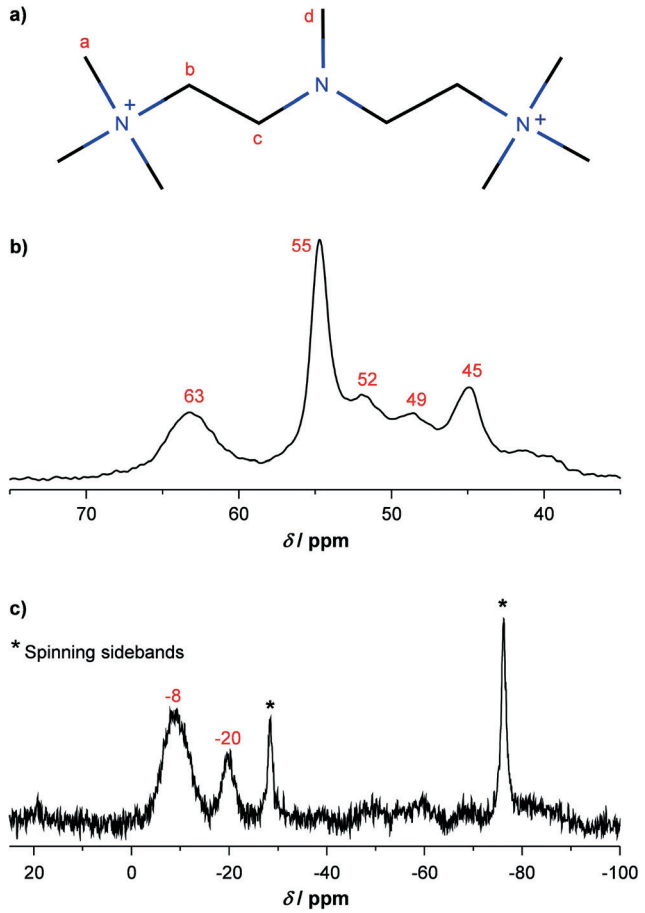

Fig. 1 a) Structure of the diquaternary cation HM-dq used as the SDA. b) ^{13}C and c) ^{19}F solid-state MAS NMR spectra of the as-synthesised Ge-BEC. The spinning side bands in (c) arise from residual SiF_6^{2-} species that give rise to a sharp peak at –123 ppm.[21,22]

the SDA was located in the pore system. To this end, we performed a full structure analysis using synchrotron X-ray powder diffraction data (XPD).

Experimental

Synthesis

SDA. Iodomethane (0.46 moles) was mixed with 500 cm^3 of absolute ethanol in a 2 L round-bottom flask. Pentamethyldiethylenetriamine (0.23 moles, Sigma-Aldrich, 99%) was mixed with 200 cm^3 of absolute ethanol, and was placed in an addition funnel. The amine solution was added dropwise to the methyl iodide. As the addition was carried out, precipitation was observed. After all of the amine had been added (1.5 h), the mixture was stirred at room temperature for an additional hour. The solid was then filtered and washed with absolute ethanol. The yield of HM-dq was 93.3%. Prior to its application, the product was converted from iodide to hydroxide form in deionised water using a hydroxide exchange resin (Dowex Marathon A, hydroxide form). The concentration of the SDA was determined by titration with an HCl solution (0.1 M).

Table 1 Gel compositions studied for syntheses with HM-dq as SDA

Gel	SiO_2	GeO_2	SDA	H_2O	HF	NH_4F
1	1	—	0.25	5	0.5	—
2	1	—	0.25	7	0.5	—
3	0.833	0.167	0.25	7	0.5	—
4	0.833	0.167	0.25	15	0.5	—
5	0.833	0.167	0.25	7	—	0.5
6	0.882	0.118	0.25	7	0.5	—

Ge-BEC. Different gel compositions with varying germanium oxide and water content and fluoride source were screened in the series of syntheses that yielded Ge-BEC (Table 1). The gel was prepared by dissolving germanium oxide in an aqueous solution of HM-dq. Then, tetraethyl orthosilicate (TEOS) was hydrolysed in the solution and the mixture stirred mechanically at room temperature until the ethanol produced was completely eliminated and the amount of water matched the desired composition. Finally, HF was added and the mixture was homogenised, prior to placing the gel in a stainless-steel Teflon-lined autoclave, where it was heated at 140 °C for 7 days under slow rotation (60 rpm). After crystallisation the final pH of the synthesis gel was 7. All solids were recovered by filtration, washed with distilled water, and dried overnight at 100 °C.

Characterisation

The amounts of Si and Ge in the solid were determined by inductively coupled plasma optical emission spectroscopy (ICP-OES) using a Horiba Ultima 2 instrument equipped with photomultiplier tube detection. Samples were dissolved in a NaOH matrix, diluted with deionised water, and measured with a 5-point calibration curve. CHN analysis was undertaken using a LECO CHN-900 analyser. The total organic content in the zeolite was estimated from the weight loss between 100–550 °C measured by thermogravimetric analysis, performed in air in a Mettler Toledo TGA/SDTA851e microbalance.

^{13}C and ^{19}F NMR measurements were conducted using a Bruker Avance 400 spectrometer at room temperature under magic angle spinning (MAS) conditions. ^{19}F spectra were acquired in 2.5 mm ZrO_2 rotors at a spinning speed of 18 kHz and a carrier frequency of 376.6 MHz using a 90° pulse with a length of 5 μs, a recycle delay of 2 s and 256 accumulations and using $CFCl_3$ as a reference. ^{13}C NMR spectra were acquired in 4 mm ZrO_2 rotors at a spinning rate of 10 kHz and a carrier frequency of 100.6 MHz using a 90° pulse with a length of 4.75 μs, a recycle delay of 5 s and 10 240 accumulations and using tetramethylsilane as a reference.

Synchrotron XPD data were collected on an as-synthesised sample of Ge-BEC in a 0.3 mm capillary on the Materials Science beamline at the Swiss Light Source (wavelength 0.6197 Å, MYTHEN II detector) in Villigen, Switzerland.[20]

Scanning electron microscopy (SEM) micrographs were acquired on a Zeiss Gemini microscope (5 kV). The powdered

sample was dispersed on carbon tape and a thin coating of Pt applied to minimise charging.

Ar sorption at −196 °C was measured in a Micromeritics 3Flex analyser after evacuation of the samples at 200 °C for 3 h. The Ge-BEC zeolite was calcined in air at 500 °C for 4 h (1 °C min^{-1} ramp rate) to remove the organic SDA prior to analysis.

Results

XPD data indicated that a highly crystalline material could be attained from gel composition 3 (Table 1). However, initial attempts to index the diffraction pattern of Ge-BEC using the auto-indexing routine in *Topas*[23] failed. By examining the diffraction patterns of a series of materials synthesised in earlier experiments, it was possible to identify several small peaks in the diffraction patterns arising from a minor impurity phase. By excluding these from the indexing procedure, the synchrotron diffraction pattern could be indexed with a tetragonal unit cell (extinction symbol *P*—*c*; a = 12.6837 Å, c = 13.1683 Å). A search of the Database of Zeolite Structures[1] for structures with similar unit cell parameters indicated that the material was likely to have a **BEC**-type framework.

Elemental analyses confirmed that the isolated material had a Si : Ge ratio similar to that used in the synthesis (5.1), while the organic content of the as-synthesised zeolite was 13.6 wt.% (Fig. S1†). The C : N ratio (3.7) agreed well with that expected for the SDA and indicates that the latter probably remained unaltered in the crystalline product. Previously, it has been suggested that HM-dq could decompose into smaller amines, which could also act as SDAs.[18] Characterisation by ^{13}C MAS NMR further corroborated the structural integrity of the large amine (Fig. 1b). In particular, the peaks at 63, 55, 52, and 45 ppm are consistent with those expected from carbon in positions b, a, c, and d of the SDA, respectively (Fig. 1a).[19] The small band at 49 ppm indicates that some of the SDA may not be in diquaternary form.

Rietveld refinement[24] was initiated in the space group $P4_2/mmc$ using the coordinates of ITQ-17[4] and the program *Topas*.[25] Geometric restraints were applied to all unique bond distances and angles. The background was removed manually and adjusted as necessary during the refinement. An approximate scale factor was determined by performing a few cycles of refinement using only the higher angle XPD data and keeping all other parameters fixed. Then a difference electron density map, generated using this scale factor for the whole pattern, revealed an electron cloud in the zeolite pores. An initial model for the SDA was created and optimised using the energy minimisation routine in *Jmol*.[26] The molecule was added to the structural model as a rigid body, and its location and orientation were optimised using the simulated annealing routine in *Topas*. Several internal torsion angles were allowed to vary to take the flexibility of the SDA into account. It settled on a position with 4-fold symmetry. Initially, the occupancy of the SDA was refined freely, but it converged quickly to approximately 0.25, so it was fixed at that value.

To account for the Ge atoms in the framework, all T atoms were redefined as mixed Si : Ge positions, each with a total occupancy of 1.0. Further refinement clearly indicated that the Ge was located in the *d4r*. Those not in the *d4r* refined close to full Si occupancy, and were consequently fixed at this value.

Although most electron density was accounted for at this point, the match of the calculated diffraction pattern to the observed one was poor, and several peaks appeared to have shoulders. With the hope that extra reflections could account for this discrepancy, the unit cell parameters were doubled in each direction (a = 25.63745 Å, c = 26.3769 Å), and the space group changed to $I4_1/amd$, as in the structure of pure Ge FOS-5.[3] In $I4_1/amd$, there are two independent *d4r* units with site symmetry 2/*m*, and two independent T atoms per *d4r*. The Ge occupancy of one T atom in particular refined to a value over 0.5. With the mirror symmetry along [100], this means that some Ge atoms would occupy neighbouring T sites. Typically, Ge and Si arrange themselves in an alternating fashion, so we changed the space group to $I4_1/a$, which has a local site symmetry of $\bar{1}$ in the *d4r* units. This enabled a more realistic distribution of the Ge atoms.

While the profile fit improved somewhat, doubling the unit cell parameters contributed little to this. The fit did not improve as drastically as expected, and the shoulders were still not explained. Furthermore, with 48 framework atoms in the asymmetric unit, overparametrisation became a problem. Therefore, the unit cell doubling was reversed, but the space group was changed to $P\bar{4}2c$, a subgroup of $P4_2/mmc$, to realise 222 symmetry in the *d4r*.

Further improvements were made by changing the SDA from a rigid-body model to a restrained one, and by introducing a model for anisotropic peak broadening.[27] Residual electron density in the middle of the *d4r* was assigned to a fluoride ion, and its occupancy refined to 0.19 per *d4r* or 0.38 per unit cell. ^{19}F MAS NMR (Fig. 1c and S2†) confirmed the presence of fluoride inside the *d4r* units. Specifically, two intense lines at −8 and −20 ppm are typical of fluoride anions in the *d4r* units in a **BEC**-type zeolite.[28] As such, further residual electron density inside the channels was tentatively assigned to hydroxide, and it refined to an occupancy of 0.301. This means the charges are not fully balanced (+4 from N^+ in the SDA *vs.* −2.8 from F^- and OH^-), but it was not possible to locate more negatively charged ions from the data directly. We must conclude that some F^- in the *d4r* and/or disordered OH^- in the pores were not located.

Only the positions T1 and T2 in the *d4r* refined with a significant amount of Ge (0.23 and 0.41). The total occupancy of Ge adds up to 5.12 per unit cell. This corresponds well to the Si : Ge molar ratio of 5.1 (5.3 Ge per unit cell) found in the elemental analysis. To account for the larger Ge–O distance of 1.73 Å, the corresponding distance restraints for T1 and T2 were increased to 1.65 Å (Table 2).

Table 2 Framework bond angles (°) and distances (Å)

	Restraint	Min.	Max.	Average
Si–O	1.61	1.59	1.62	1.60
(Si/Ge)–O	1.65	1.65	1.66	1.65
O–Si–O	109.5	106.3	113.2	109.5
O–(Si/Ge)–O	109.5	104.3	113.8	109.4
Si–O–Si	145	149.1	163.4	156.4
Si–O–(Si/Ge)	145	140.5	149.3	145.0
(Si/Ge)–O–(Si/Ge)	145	137.6	144.8	141.2

All atomic positions were refined with isotropic displacement parameters using scattering factors for neutral atoms. H atoms in the SDA were taken into account by increasing the population factors of the corresponding C atoms to account for the extra electrons. The final difference electron density map had some residual electron density around the *d*4*r*, which can be attributed to the static disorder resulting from the mixed Si/Ge sites. We tried to model the density by refining independent sites for each Ge and Si atom, but this did not improve the profile fit, so the simpler model was used for the final refinement. Details of the refinement are given in Table 3, and the profile fit is shown in Fig. 2.

Examination of the zeolite morphology by SEM, reveals that the Ge-BEC forms as twinned isometric crystals that appear to consist of an agglomeration of 50–100 nm crystallites arranged in an unusual three-dimensional cross shape (Fig. 3). Interestingly, under close inspection three independent growth directions that meet at the centre of each cross can be seen.

We hypothesise that the irregular peak shape could be attributed to stress or strain at the twin boundaries. The change of growth direction at the interface can be described as a rotation around the *a* or *b*-axis, to generate a transition layer similar to that found in the structure of ITQ-7 (**ISV**),[29] which contains an ordered stacking of such layers.

Argon sorption at 77 K was studied to verify the micropore volume and diameter in the calcined sample (Fig. 4). The Type I isotherm and the NLDFT (non-local density functional theory) derived micropore diameter of 0.73 nm are in close agreement with the observations expected for a purely microporous **BEC**-type zeolite. A micropore volume of 0.17 $cm^3\ g^{-1}$ and an external surface area of 30 $m^2\ g^{-1}$ were derived by application of the *t*-plot, which is in good agreement with previous reports in the literature.[14]

Table 3 Crystallographic data for Ge-BEC

Composition	$\lvert(C_{11}H_{29}N_3)_2(OH)_{2.4}F_{0.4}\rvert[Si_{26.9}Ge_{5.1}O_{64}]$
Space group	$P\bar{4}2c$
a (Å)	12.6710(8)
c (Å)	13.1674(9)
V (Å^3)	2114.1(3)
2θ range (°)	1.3–40.3
λ (Å)	0.61965(1)
R_I	0.092
R_{wp}	0.236
R_{exp}	0.020
GOF	11.57
Observations	10828
Reflections	917
Parameters	100
Geometric restraints	80

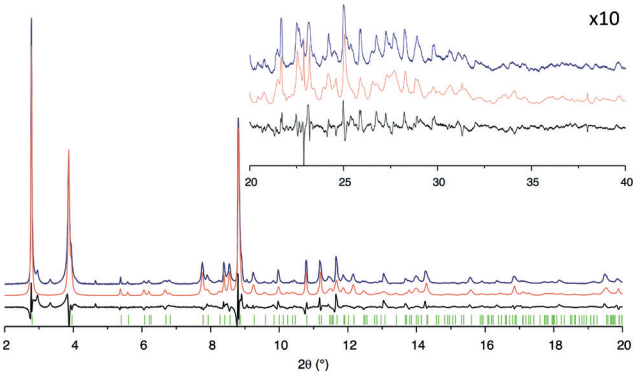

Fig. 2 Observed (blue), calculated (red), and difference (black) profiles for the Rietveld refinement. The high angle data shown in the inset have been multiplied by 10 to facilitate visualisation.

Discussion

Although the final R_{wp} of 0.235 for the profile fit is rather high, most of the differences are for the three largest diffraction peaks, for which the peak shape was difficult to reproduce. However, the Ge content and arrangement were confirmed independently *via* elemental analysis and ^{19}F MAS NMR, respectively. The reliability of the refinement is also reflected in the R_I value of 0.092, which is indicative of a reasonable agreement between the observed and calculated diffraction intensities.

In the refined structure, the SDA is disordered around a 4-fold axis in the centre of the 12-ring channels, aligned approximately along the [100] or [010] directions (Fig. 5). Each SDA molecule can thus adopt any one of four different

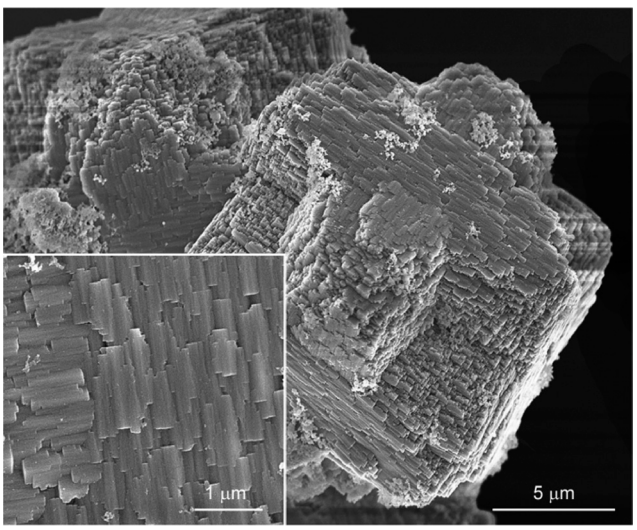

Fig. 3 SEM image showing the morphology of Ge-BEC.

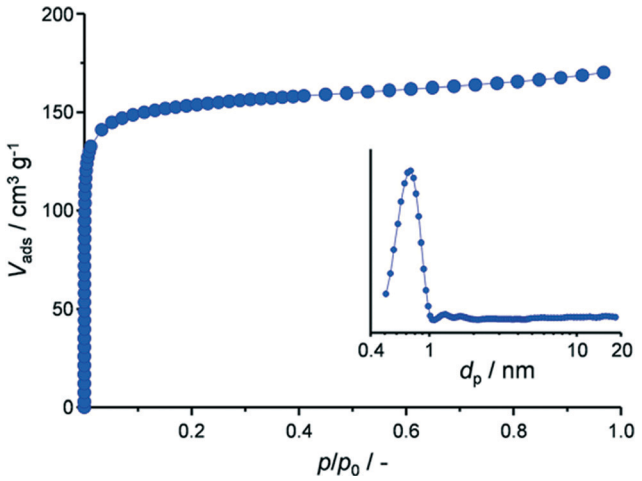

Fig. 4 Ar isotherm at 77 K and the corresponding NLDFT pore size distribution (inset) of calcined Ge-BEC.

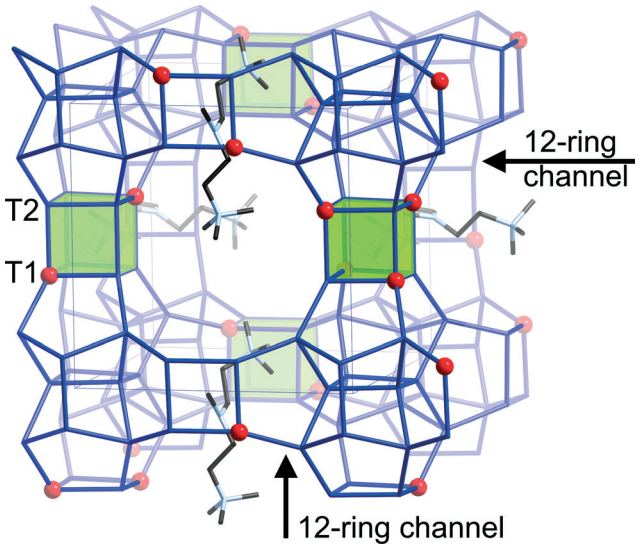

Fig. 5 The **BEC**-type framework structure of Ge-BEC viewed along the [001] direction showing the arrangement of the *d4r* units (green), a possible arrangement of Ge in the *d4r* (red), and the positions of the SDAs in the channels. Note that all Ge atoms are in *d4r* units.

positions in any given unit cell. The SDA fits well within the channel system and is slightly displaced towards the channel intersection. This can be represented nicely with a Hirshfeld surface[30] (Fig. 6). Here, blue represents areas with long intermolecular contacts (*i.e.* the contact distance is greater than the sum of the van der Waals radii), and red represents short intermolecular contacts (*i.e.* shorter than the sum of the van der Waals radii). The positive charges are located at both ends of the SDA, and in this orientation, the positively charged quaternary ammonium is close to the *d4r*, where the negatively charged fluoride ion is located. At the other end, there is a loosely associated hydroxide ion. All short contact distances are greater than 3.0 Å. The shortest C–O distances

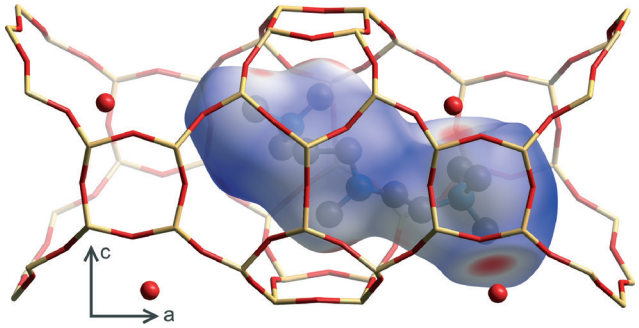

Fig. 6 Cavity in Ge-BEC showing the Hirshfeld surface[30] of the SDA and the positions of the associated hydroxide ions.

are 3.01(2) Å between C9 and O9, 3.04(1) Å between C4 and O5, 3.07(1) Å between C6 and O1, and 3.10(2) Å between C10 and O1.

The location of the SDA here is similar to that found in FOS-5.[3] In that case, the authors assumed that the DABCO SDA had broken down into individual Me_3N molecules, although the intermolecular distances and orientation of the moieties are very much in line with what could be expected for DABCO. The DABCO or Me_3N molecules in FOS-5, and the HM-dq in Ge-BEC are both located in the middle of the 12-membered rings along *a* and *b*. It appears that the SDA is necessary to stabilise the formation of the 12-rings in these directions.

Conclusions

A zeolite beta polymorph C material with low Ge content has been synthesised successfully using a flexible SDA and its structure analysed using synchrotron XPD data. The location of Ge and extra-framework species could be determined by combining Rietveld refinement with simulated annealing and difference Fourier analyses. As in other studies of germanosilicates with low Ge content, the Ge was found to be located preferentially in the *d4r*'s.

Although **BEC**-type germanosilicates have been synthesised with a Si : Ge ratio of up to 30, only a material with a Si : Ge ratio of 1.8 has been subjected to structure analysis.[4] In that case, Ge was found to be approximately twice as likely to occupy the T-sites in the *d4r* as other sites. Here we have shown that for polymorph C with a Si : Ge ratio of 5.1, Ge is found exclusively in the *d4r* units.

The initial position of the flexible SDA could be determined using a simulated annealing approach. We have used this method in other studies to locate starting positions for rigid SDA molecules in zeolite channels,[31–33] but it seems that with careful handling, it can also be applied to more flexible moieties.

Acknowledgements

We thank Antonio Cervellino for his assistance with the powder diffraction measurements on the Materials Science

Beamline at the SLS in Villigen, Switzerland. Funding from the Swiss National Science Foundation is gratefully acknowledged. Drs. Karsten Kunze (ScopeM, ETH) and René Verel (NMR service, ETH) are thanked for assistance with the SEM and NMR measurements, respectively. The Micromeritics grant program is thanked for the award of the 3Flex.

References

1 Three-letter framework type codes (boldface capital letters) for all zeolites mentioned in the text are given in parenthesis. They can be found in: C. Baerlocher, L. B. McCusker and D. H. Olson, *Atlas of Zeolite Framework Types*, Elsevier, Amsterdam, 6th edn, 2007.
2 J. M. Newsam, M. M. J. Treacy, W. T. Koetsier and C. B. D. Gruyter, *Proc. R. Soc. London, Ser. A*, 1988, **420**, 375–405.
3 T. Conradsson, M. S. Dadachov and X. Zou, *Microporous Mesoporous Mater.*, 2000, **41**, 183–191.
4 A. Corma, M. T. Navarro, F. Rey, J. Rius and S. Valencia, *Angew. Chem.*, 2001, **113**, 2337–2340.
5 Z. Liu, T. Ohsuna, O. Terasaki, M. A. Camblor, M.-J. Díaz-Cabañas and K. Hiraga, *J. Am. Chem. Soc.*, 2001, **123**, 5370–5371.
6 Á. Cantín, A. Corma, M. J. Díaz-Cabañas, J. L. Jordá, M. Moliner and F. Rey, *Angew. Chem., Int. Ed.*, 2006, **45**, 8013–8015.
7 M. Moliner, P. Serna, Á. Cantín, G. Sastre, M. J. Díaz-Cabañas and A. Corma, *J. Phys. Chem. C*, 2008, **112**, 19547–19554.
8 A. Corma and M. E. Davis, *ChemPhysChem*, 2004, **5**, 304–313.
9 T. Blasco, A. Corma, M. J. Díaz-Cabañas, J. L. Jordá, F. Rey, J. A. Vidal-Moya and C. M. Zicovich-Wilson, *J. Phys. Chem. B*, 2002, **106**, 2634–2642.
10 G. Sastre, A. Pulido, R. Castañeda and A. Corma, *J. Phys. Chem. B*, 2004, **108**, 8830–8835.
11 P. Kamakoti and T. A. Barckholtz, *J. Phys. Chem. C*, 2007, **111**, 3575–3583.
12 F. Gao, M. Jaber, K. Bozhilov, A. Vicente, C. Fernandez and V. Valtchev, *J. Am. Chem. Soc.*, 2009, **131**, 16580–16586.
13 H. Xu, J.-G. Jiang, B. Yang, L. Zhang, M. He and P. Wu, *Angew. Chem.*, 2014, **126**, 1379–1383.
14 M. El-Roz, L. Lakiss, A. Vicente, K. N. Bozhilov, F. Thibault-Starzyk and V. Valtchev, *Chem. Sci.*, 2014, **5**, 68–80.
15 E. Verheyen, L. Joos, K. Van Havenbergh, E. Breynaert, N. Kasian, E. Gobechiya, K. Houthoofd, C. Martineau, M. Hinterstein, F. Taulelle, V. Van Speybroeck, M. Waroquier, S. Bals, G. Van Tendeloo, C. E. A. Kirschhock and J. A. Martens, *Nat. Mater.*, 2012, **11**, 1059–1064.
16 M. Shamzhy, M. Opanasenko, Y. Tian, K. Konysheva, O. Shvets, R. E. Morris and J. Čejka, *Chem. Mater.*, 2014, **26**, 5789–5798.
17 P. Chlubná-Eliášová, Y. Tian, A. B. Pinar, M. Kubů, J. Čejka and R. E. Morris, *Angew. Chem.*, 2014, **126**, 7168–7172.
18 P. Feng, X. Bu and G. D. Stucky, *Nature*, 1997, **388**, 735–741.
19 A. Moini, K. D. Schmitt and R. F. Polomski, *Zeolites*, 1997, **18**, 2–6.
20 A. Bergamaschi, A. Cervellino, R. Dinapoli, F. Gozzo, B. Henrich, I. Johnson, P. Kraft, A. Mozzanica, B. Schmitt and X. Shi, *J. Synchrotron Radiat.*, 2010, **17**, 653–668.
21 H. Kessler, J. Patarin and C. Schott-Darie, in *Stud. Surf. Sci. Catal.*, ed. M. Stöcker, H. G. Karge, J. C. Jansen and J. Weitkamp, Elsevier, 1994, vol. 85, pp. 75–113.
22 S. I. Zones, R. J. Darton, R. Morris and S.-J. Hwang, *J. Phys. Chem. B*, 2005, **109**, 652–661.
23 A. A. Coelho, *J. Appl. Crystallogr.*, 2003, **36**, 86–95.
24 H. M. Rietveld, *J. Appl. Crystallogr.*, 1969, **2**, 65–71.
25 A. A. Coelho, *TOPAS-ACADEMIC v5.0*, 2012.
26 R. M. Hanson, *J. Appl. Crystallogr.*, 2010, **43**, 1250–1260.
27 P. W. Stephens, *J. Appl. Crystallogr.*, 1999, **32**, 281–289.
28 J. A. Vidal-Moya, T. Blasco, A. Corma, M. T. Navarro and F. Rey, *Stud. Surf. Sci. Catal.*, 2004, **154, Part B**, 1289–1294.
29 L. A. Villaescusa, P. A. Barrett and M. A. Camblor, *Angew. Chem., Int. Ed.*, 1999, **38**, 1997–2000.
30 M. A. Spackman and D. Jayatilaka, *CrystEngComm*, 2009, **11**, 19–32.
31 S. Smeets, D. Xie, L. B. McCusker, C. Baerlocher, S. I. Zones, J. A. Thompson, H. S. Lacheen and H.-M. Huang, *Chem. Mater.*, 2014, **26**, 3909–3913.
32 S. Smeets, D. Xie, C. Baerlocher, L. B. McCusker, W. Wan, X. Zou and S. I. Zones, *Angew. Chem.*, 2014, **126**, 10566–10570.
33 S. Smeets, L. B. McCusker, C. Baerlocher, D. Xie, C. Y. Chen and S. I. Zones, *J. Am. Chem. Soc.*, 2015, **137**, 2015–2020.

